Interface Double-Exchange Ferromagnetism in the Mn-Zn-O System: New Class of Biphase Magnetism

M. A. García,[1,2] M. L. Ruiz-González,[3] A. Quesada,[1,2] J. L. Costa-Krämer,[4] J. F. Fernández,[5] S. J. Khatib,[6] A. Wennberg,[4] A. C. Caballero,[5] M. S. Martín-González,[4] M. Villegas,[5] F. Briones,[4] J. M. González-Calbet,[1,3] and A. Hernando[1,2,*]

[1]*Instituto de Magnetismo Aplicado (RENFE-UCM-CSIC), P.O. Box 155, 28230 Las Rozas, Madrid, Spain*
[2]*Departamento de Física de Materiales, UCM, 28040 Madrid, Spain*
[3]*Departamento de Química Inorgánica I, UCM, 28040 Madrid, Spain*
[4]*Instituto de Microelectrónica de Madrid, CNM-CSIC, Isaac Newton 8 PTM, 28760 Tres Cantos, Madrid, Spain*
[5]*Instituto de Cerámica y Vidrio, CSIC, Cantoblanco, 28049 Madrid, Spain*
[6]*Instituto de Catálisis y Petroleoquímica, CSIC, Cantoblanco, 28049 Madrid, Spain*

(Received 9 February 2005; published 3 June 2005)

In this Letter, we experimentally show that the room temperature ferromagnetism in the Mn-Zn-O system recently observed is associated with the coexistence of Mn^{3+} and Mn^{4+} via a double-exchange mechanism. The presence of the ZnO around MnO_2 modifies the kinetics of $MnO_2 \rightarrow Mn_2O_3$ reduction and favors the coexistence of both Mn oxidation states. The ferromagnetic phase is associated with the interface formed at the Zn diffusion front into Mn oxide, corroborated by preparing thin film multilayers that exhibit saturation magnetization 2 orders of magnitude higher than bulk samples.

DOI: 10.1103/PhysRevLett.94.217206 PACS numbers: 75.50.Pp, 75.70.Cn, 82.33.Pt

Prompted by the need to understand the unusual magnetic properties recently observed in the Mn-Zn-O system, considerable work has been carried out. The first observation of room temperature (RT) ferromagnetism (FM) was reported by Sharma *et al.* [1] in low Mn content (10%MnO_2–90%ZnO and 2%MnO_2–98%ZnO) pellets annealed at 500 °C. The ferromagnetic behavior was first explained in terms of the formation of Mn-doped ZnO, which was previously predicted to be a dilute magnetic semiconductor with a Curie temperature above 300 K [2]. However, the origin of the reported ferromagnetic behavior is still a matter of controversy. Kundaliya *et al.* [3], based on thermogravimetric analysis (TGA) experiments, suggested an oxygen-vacancy $Mn_{2-x}Zn_xO_{3-\delta}$ phase as responsible for the observed RT FM. Moreover, recent studies evidence the absence of magnetic order in Mn-doped ZnO down to 2 K [4,5]. In a recent paper [6], RT FM was confirmed in samples prepared following Sharma *et al.* method, although differences concerning the structural characterization have been found. Actually, only a weak Zn diffusion into MnO_2 grains is observed, whereas the presence of Mn into the ZnO matrix is never detected. In any case, the mechanism responsible for the RT FM has not been elucidated yet. In this sense, the aim of this work is focused on the study of the origin of the RT FM in the Mn-Zn-O system.

2%MnO_2–98%ZnO and 10%MnO_2–90%ZnO pellets were prepared following the method described by Sharma *et al.* [1,6]. Pure MnO_2 samples were also studied for comparison purposes. These samples were annealed in air at different temperatures in the range 500 °C–800 °C for 12 h. After annealing at 500 °C, the ZnO-MnO_2 samples exhibit RT ferromagnetic behavior, as previously reported [6].

The x-ray diffraction pattern shown in Fig. 1(a) and corresponding to the 10%MnO_2–90%ZnO sample can be indexed on the basis of a mixture phase constituted by a majority one (ZnO), one minority, around 5% (Mn_2O_3), and traces of MnO_2 and $Zn_xMn_{3-x}O_4$. This result can be understood taking into account that MnO_2 can be partially reduced to Mn_2O_3 when treated at 500 °C, the temperature at which a total diffusion of Zn into Mn oxide grains is far from being reached. On the other hand, it is well known that x-ray diffraction (XRD) supplies average structural information. This means that if local diffusion of Mn in Zn has happened it could not be detected by this technique. In this sense, a transmission electron microscopy study linked with energy-dispersive x-ray spectroscopy (EDS) analysis has been performed to check if any local diffusion has succeeded. This information would be, indeed, very valuable in order to understand the observed magnetic properties. EDS analysis shows the presence of particles exhibiting different composition. The majority ones contain only Zn, while around 5% involves only Mn. A third type, in a very low ratio, comprising both cations, also appears. Selected area electron diffraction (SAED) patterns of the particles containing Mn and Zn separately can be, respectively, indexed on the basis of the ZnO and Mn_2O_3 unit cells, in agreement with the XRD study. On the other hand, particles containing both cations display Mn/Zn average ratios between 2.5 and 4. Moreover, inside each crystal changes in the Mn/Zn ratio are apparent. The SAED and the high resolution electron microscopy (HREM) study suggest that in each region containing Mn and Zn a spinel-like structure is stabilized. As a representative example, for a Mn/Zn = 2.5 ratio, a HREM image and its corresponding fast Fourier transform (FFT) along the $[\bar{1}31]$ zone axis are displayed in Fig. 1(b).

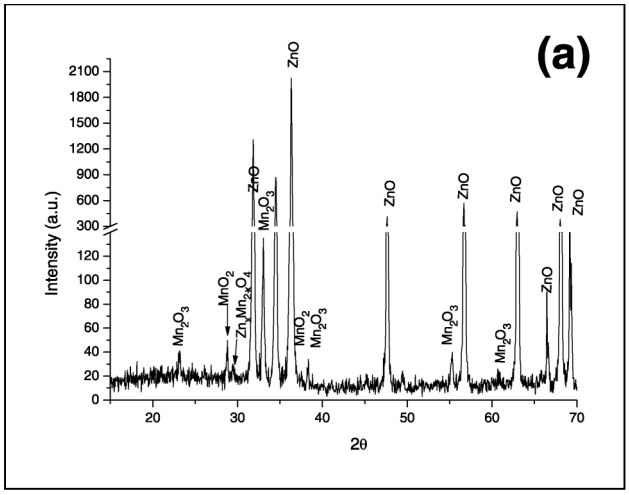

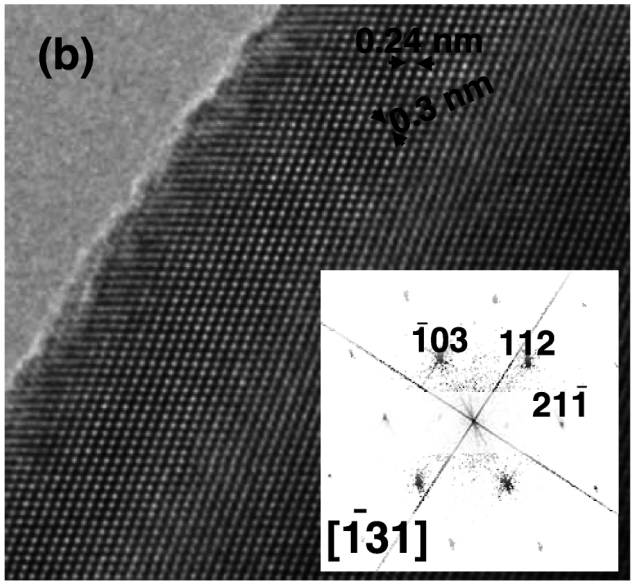

FIG. 1. (a) XRD pattern corresponding to the 10%MnO_2–90%ZnO sample. Peaks can be indexed and labeled on the basis of the mixture of ZnO, Mn_2O_3, MnO_2, and $Zn_xMn_{3-x}O_4$. (b) HREM image of a crystal containing both Zn and Mn cations along the $[\bar{1}31]$ zone axis. Periodicities are in agreement with a spinel cell. Inset shows the corresponding FFT.

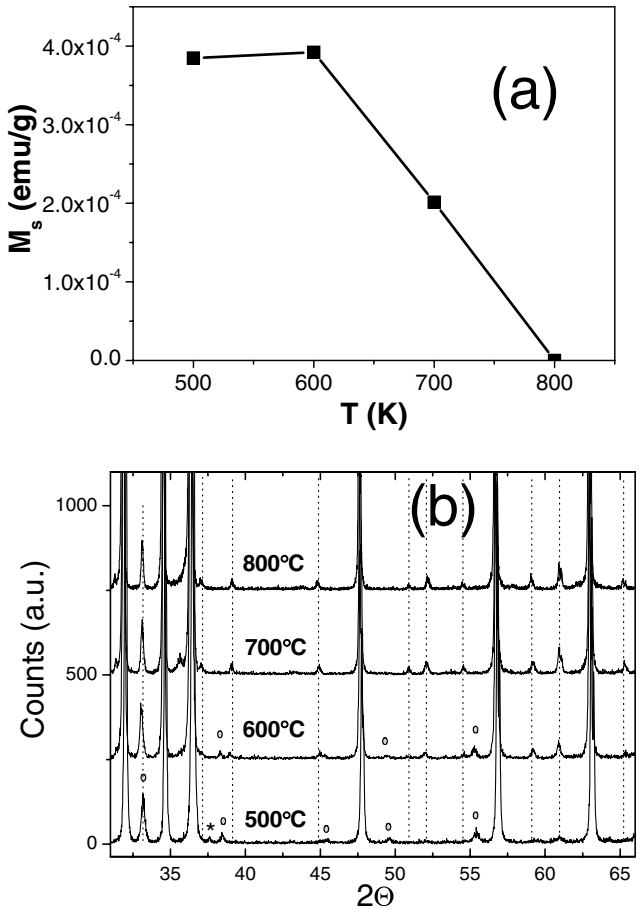

FIG. 2. Evolution of (a) M_s and (b) XRD patterns with the annealing temperature from the 10%MnO_2–90%ZnO sample. Dashed lines, circles, and asterisk represent the main peaks from $Zn_xMn_{3-x}O_4$, Mn_2O_3, and MnO_2, respectively.

Changes in the microstructure were not found on particles having different Mn/Zn ratios, suggesting that a solid solution $Zn_xMn_{3-x}O_4$ ($0 \leq x \leq 1$) can be formed when MnO_2 and ZnO are heated up together. It is remarkable that the Zn content is never found to be $x \geq 1$; i.e., the spinel phase is always Mn rich. On the other hand, it is clear that the proportion of this phase is very low, in agreement with x-ray diffraction information. Evidence of Mn-doped ZnO was not detected.

Increasing the annealing temperature above 600 °C gives rise to a decrease of the FM signal at room temperature that completely disappears after annealing at 800 °C [Fig. 2(a)], in agreement with previous studies [1]. The XRD patterns of the annealed samples displayed in Fig. 2(b) indicate structural changes. Above 500 °C, the very weak signal corresponding to MnO_2 disappears while the Mn_2O_3 peak intensity starts decreasing. In addition, new peaks characteristic of a spinel-like phase, $Zn_xMn_{3-x}O_4$, appear and their intensities increase as the temperature is enhanced. The HREM study of the sample treated at 800 °C confirms a Zn rich spinel structure, suggesting that heating has allowed further diffusion of Zn. The simultaneous increase of the $Zn_xMn_{3-x}O_4$ phase and decrease of the ferromagnetic signal suggests that this phase is not responsible for the RT FM. Although there is some controversy about the magnetic properties of this spinel, it is well known that it exhibits paramagnetic behavior at RT [7]. For a further understanding, several samples in the $Zn_xMn_{3-x}O_4$ system have been prepared and characterized. FM at RT was never observed in this solid solution.

Since no manganese oxides are ferromagnetic at room temperature, the observed FM must be related to the reaction of MnO_2 with ZnO prior to the final formation of the $Zn_xMn_{3-x}O_4$ spinel. The kinetics of MnO_2 reduction is

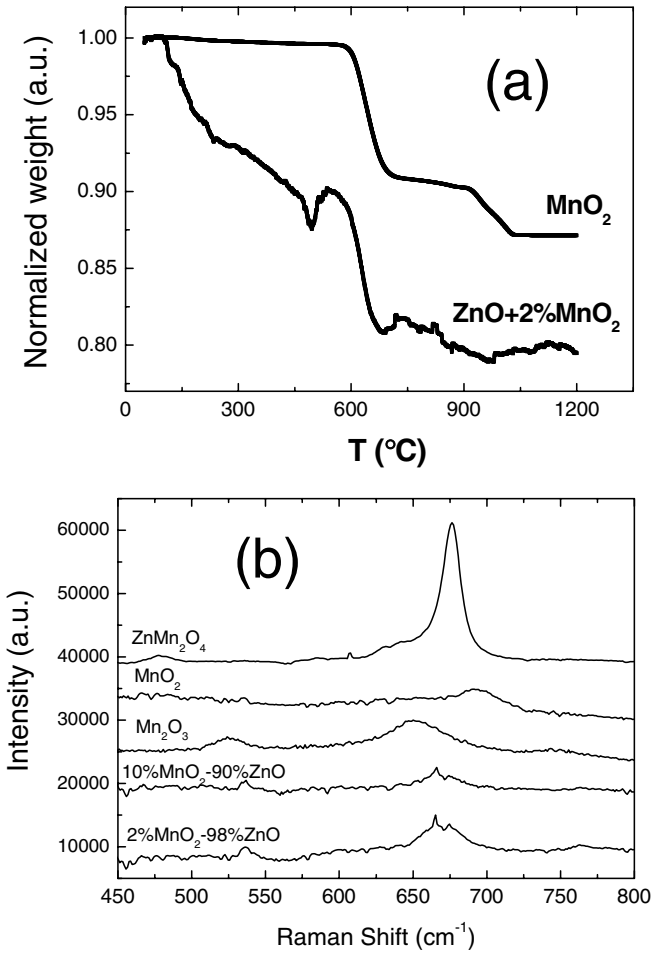

FIG. 3. (a) TGA from pure MnO_2 and the component of MnO_2 in 2%MnO_2–98%ZnO. The latter was obtained by subtracting the data for pure ZnO from the experimental results. (b) Raman spectra from 2%MnO_2–98%ZnO, 10%MnO_2–90%ZnO, MnO_2, Mn_2O_3, and $ZnMn_2O_4$.

modified by the presence of Zn. In this sense, TGA [Fig. 3(a) and also Fig. 2(b) of Ref. [3]] shows that the $MnO_2 \rightarrow Mn_2O_3$ reduction process ($Mn^{4+} \rightarrow Mn^{3+}$) is very sharp and takes place between 500 °C and 600 °C. However, in the presence of Zn, $Mn^{4+} \rightarrow Mn^{3+}$ reduction starts at lower temperature (about 200 °C) and there is a progressive reduction up to 600 °C. Therefore, the temperature range where Mn^{3+} and Mn^{4+} coexist is wider in the presence of Zn.

In order to get more reliable information of manganese oxidation states, Raman studies were performed. Raman spectra of 2%MnO_2–98%ZnO and 10%MnO_2–90%ZnO samples annealed at 500 °C as well as those corresponding to references are displayed in Fig. 3(b). Raman modes from MnO_2 and Mn_2O_3 in the 600–700 cm^{-1} region appear at 645 and 690 cm^{-1}, respectively. The ferromagnetic samples show two overlapping peaks in this region at 674 and 659 cm^{-1}. The former is characteristic of the spinel phase; the latter is related to an intermediate oxidation state [8], that is, local coexistence of Mn^{+4} and Mn^{+3}. In our case, the presence of Zn seems to stabilize this mixture of oxidation states.

It is worth noting that the RT FM is found only for the latter samples annealed in the temperature range where Mn^{3+} and Mn^{4+} coexist, pointing to the simultaneous presence of both oxidation states as responsible for the observed RT FM. The coexistence of Mn^{3+} and Mn^{4+} is known to be responsible for FM via the double-exchange mechanism in different compounds [9,10], which usually exhibits a large Curie temperature (T_C) even above RT [11]. Actually, the situation is similar to that found in $La_{1-x}Ca_xMnO_3$. For $x = 1$ the valence of Mn is 4+, whereas for $x = 0$ the valence is 3+. None of those compounds is FM, but the intermediate values of x, which yield to a mixture of Mn^{3+} and Mn^{4+}, give rise to the appearance of FM with high T_C.

It has not been described yet how the presence of Zn modifies the kinetics of MnO_2 reduction. During the annealing process, Zn diffuses into MnO_2 grains favoring the reduction to Mn_2O_3 and subsequent formation of the $Zn_xMn_{3-x}O_4$. This is clearly observed by EDS microanalysis, since different areas of the same particle show changes in the Mn/Zn ratio. The Mn^{3+} oxidation state seems to be associated with phases containing Zn that are doped Mn_2O_3 and $Zn_xMn_{3-x}O_4$, whereas Mn^{4+} is in MnO_2. Therefore, it is expected that both Mn^{3+} and Mn^{4+} coexist in the interface which separates regions with Zn from those without Zn, that is, the Zn diffusion front into Mn oxide grains. Figure 4 summarizes this situation. This would explain the low saturation magnetization value reported [1,3,6] in the RT ferromagnetic bulk systems, and that the ferromagnetic phase is observed over a large paramagnetic component but it has not been reported as isolated: FM is not associated with a phase but with the interface between nonferromagnetic phases.

In order to confirm this point, we have tried to increase the MnO_2/ZnO interface (and therefore the surface of the Zn diffusion front) by growing a thin film multilayer sample consisting of 40 sequential ZnO/MnO_2 bilayers by pulsed laser deposition onto a Si substrate. The ZnO and MnO_2 individual layers are 7.5 and 1.5 nm thick, respectively. The hysteresis loops of this sample are shown in Fig. 4(b). The saturation magnetization is 1 emu/cm^3, 2 orders of magnitude larger than the highest M_s reported for this system in bulk, and similar to the best value reported for thin films [12], confirming that the FM is originated at the interface. The coercive force for this sample [around 50 Oe at 5 K as shown in the inset of Fig. 4(b)] is smaller than for bulk material (180 Oe at 5 K) [6]. Thereby, further analysis of the anisotropy and technical magnetization processes in these multilayers must be carried out. Despite the small size of the magnetic entities, a noticeable contribution of superparamagnetic regions to the magnetization can

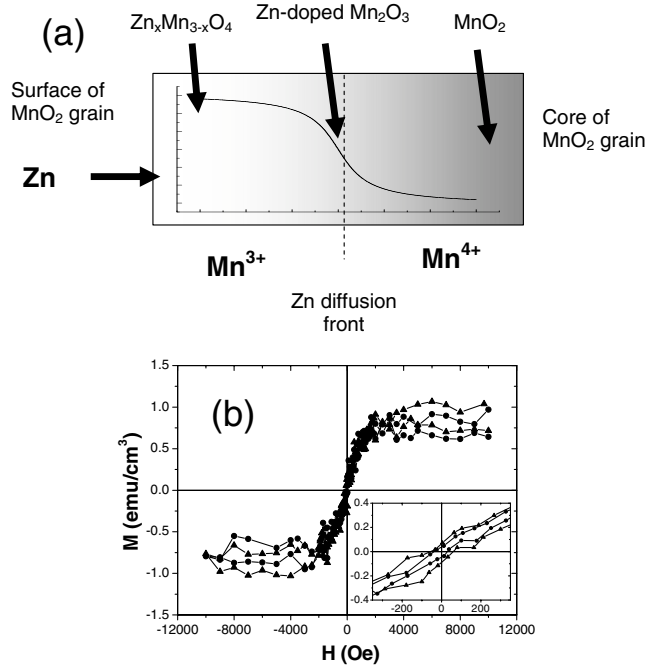

FIG. 4. (a) Scheme of the different phases at the Mn oxide grains after annealing at 500 °C and the oxidizing states of Mn. The graph indicates the concentration profile of Zn inside the grain. (b) Hysteresis loops from a 40 MnO_2/ZnO multilayer prepared by laser ablation at 5 K (triangles) and 300 K (circles). Inset shows a detail of the loops at low H. The paramagnetic-diamagnetic component has been subtracted to clearly show the FM phase.

be disregarded since, in that case, the hysteresis loops at 5 and 300 K shown in Fig. 4(b) should be fairly different (both curves should overlap when represented as a function of H/T). The XRD patterns from this sample showed a clear signal from Mn_2O_3, confirming that this phase is involved in the interface that give rises to the ferromagnetic behavior. The composition of this interface could be similar to that proposed by Kundaliya *et al.* [3].

In summary, we showed that RT FM in the Mn-Zn-O system is due to the incorporation of Zn into the MnO_2 grains. The presence of Zn modifies the kinetics of thermal reduction $Mn^{4+} \rightarrow Mn^{3+}$ during the annealing process, favoring the coexistence of both oxidation states, which gives rise to a double-exchange mechanism, responsible for the RT ferromagnetic behavior. Annealing above 500 °C increases Zn diffusion on manganese oxides, leading to spinel $Zn_xMn_{3-x}O_4$ phases. The FM arises at the interface or Zn diffusion front, and it can be increased by maximizing the interface preparing multilayers. This is a new class of surface magnetism: double-exchange mechanism, at the interface between two compounds containing Mn atoms in different oxidation states.

This work has been partially supported by the University Complutense Project No. PR1/05-13325. Partial support from the EU Network of Excellence SANDIE is also acknowledged.

*Corresponding author.
Electronic address: ahernando@renfe.es

[1] P. Sharma *et al.*, Nat. Mater. **2**, 673 (2003).
[2] T. Dietl, H. Ohno, F. Matsukura, J. Cibert, and D. Ferrand, Science **287**, 1019 (2000).
[3] D. Kundaliya *et al.*, Nat. Mater. **3**, 709 (2004).
[4] G. Lawes, A. S. Risbud, A. P. Ramírez, and R. Seshadri, Phys. Rev. B **71**, 045201 (2005).
[5] C. N. R. Rao and F. L. Deepak, J. Mater. Chem. **15**, 573 (2005).
[6] J. L. Costa-Krämer *et al.*, Nanotechnology **16**, 214 (2005).
[7] S. Asbrink *et al.*, Phys. Rev. B **60**, 12 651 (1999).
[8] C. B. Azzoni, Solid State Commun. **112**, 375 (1999).
[9] M. B. Salamon and M. Jaime, Rev. Mod. Phys. **73**, 583 (2001).
[10] J. Alonso *et al.*, Phys. Rev. B **64**, 172410 (2001).
[11] T. Okuda *et al.*, Phys. Rev. Lett. **81**, 3203 (1998).
[12] N. Theodoropoulou *et al.*, cond-mat/0408294.